

Supporting Information

**Porous Coordination Polymer-Stabilized Rhodium Single-Atom Catalyst for
Regioselective Hydroformylation**

Huiying Liao,^a Ji Ding,^a Jiaming Wang,^b Xiuge Zhao,^a Enting Shi,^a Sheng Dai,^{b,*} Haijing
Wang,^{c,*} Zhenshan Hou^{a,*}

^aState Key Laboratory of Green Chemical Engineering and Industrial Catalysis, Research Institute of Industrial Catalysis, School of Chemistry & Molecular Engineering, East China University of Science and Technology, Shanghai 200237, China.

^bKey Laboratory for Advanced Materials and Feringa Nobel Prize Scientist Joint Research Center, Institute of Fine Chemicals, School of Chemistry & Molecular Engineering, East China University of Science and Technology, Shanghai 200237, China.

^cState Key Laboratory of Petroleum Molecular & Process Engineering, SINOPEC Research Institute of Petroleum Processing Co., Ltd., Beijing 100083, China.

*Corresponding author:

E-mail: wanghaijing.ripp@sinopec.com (H. Wang); shengdai@ecust.edu.cn (S. Dai);
houzhenshan@ecust.edu.cn (Z. Hou)

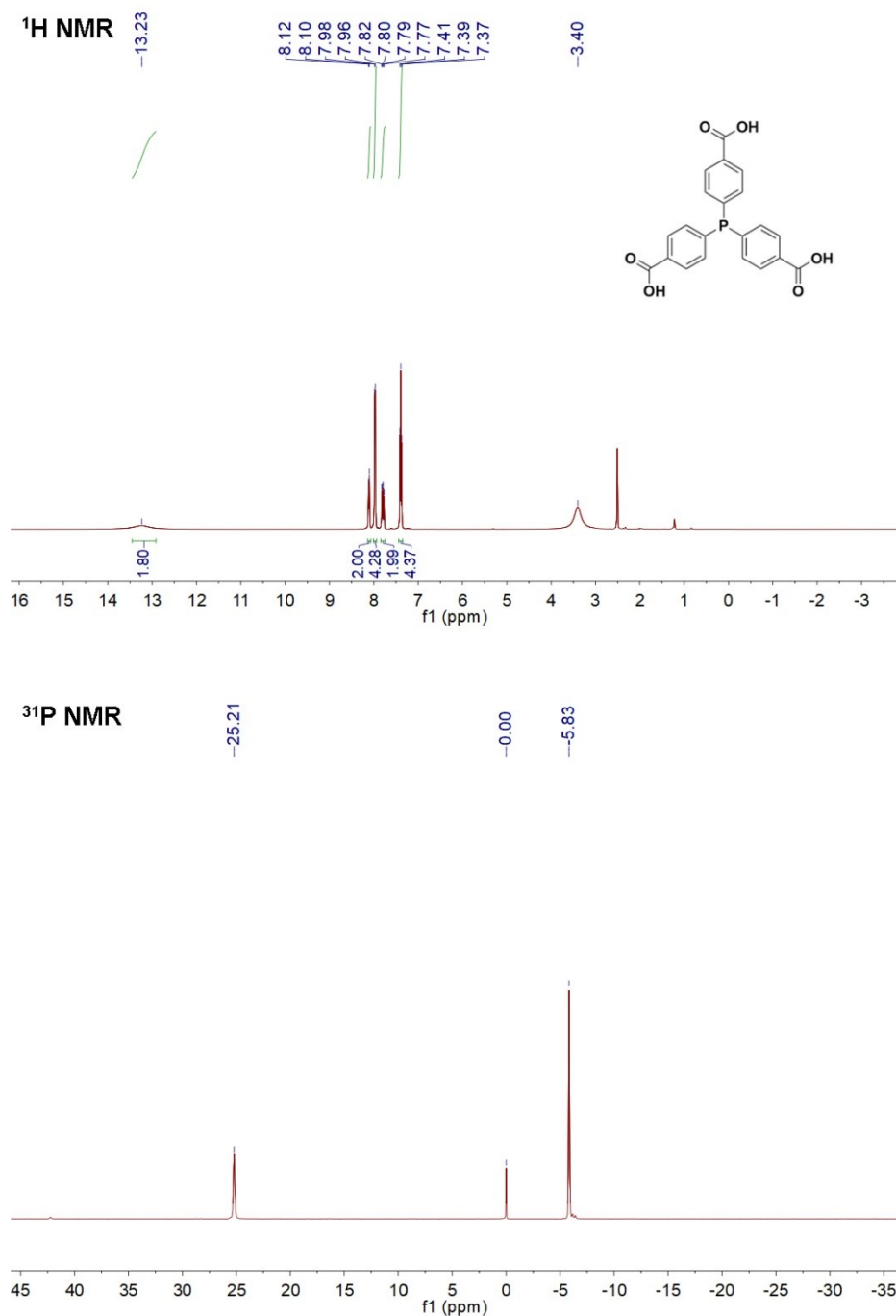


Fig. S1. The ¹H NMR and ³¹P NMR of tri(*p*-tolyl)phosphine. ¹H NMR (400 MHz, DMSO-*d*₆): δ = 13.23 (s, 2H), 8.14-8.07 (m, 2H, arom), 7.97 (d, 4H, arom., *J* = 7.1 Hz), 7.83-7.75 (m, 2H, arom.), 7.39 (t, 4H, arom., *J* = 7.8 Hz). ³¹P NMR (243 MHz, DMSO-*d*₆): δ = -5.83 (s, 1P).

Table S1. ICP-OES analysis of the catalysts.

Catalysts	Rh (wt%)
0.08Rh/Zr-HTP	0.08
0.19Rh/Zr-HTP	0.19
0.54Rh/Zr-HTP	0.54
0.92Rh/Zr-HTP	0.92

Table S2. Fitting parameters of solid-state ^{31}P NMR.

Catalysts	P species	Chemical shift (ppm)	Peak area	Percentage (%)
0.19Rh/Zr-HTP	uncoordinated P	-7.4	6.35×10^9	63.9
	P=O	25.2	2.13×10^9	21.5
	P-Rh	33.4	1.45×10^9	14.6
Zr-HTP	uncoordinated P	-7.4	6.27×10^9	71.7
	P=O	25.2	2.48×10^9	28.3

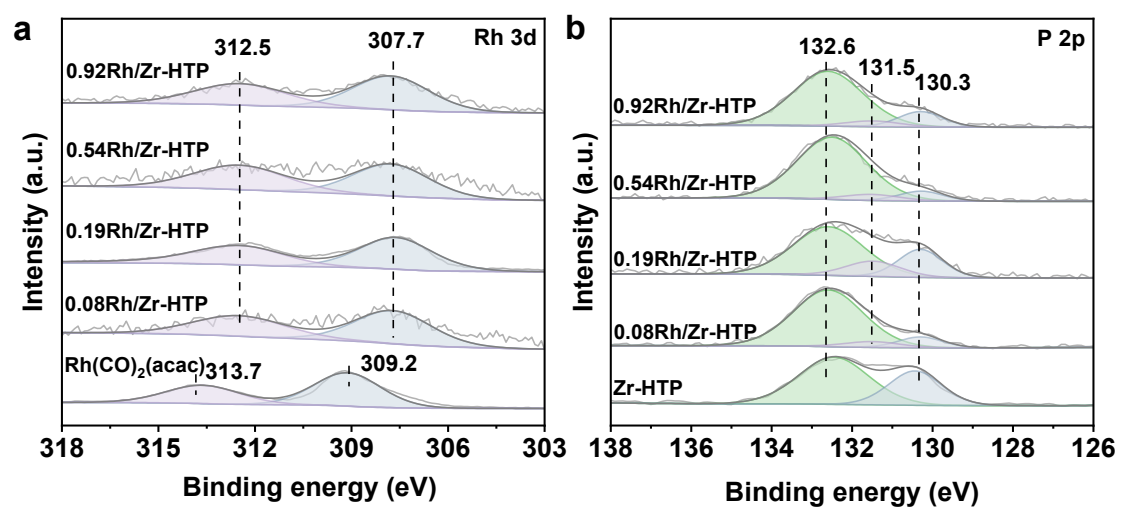


Fig. S2. The XPS spectra of different catalysts.

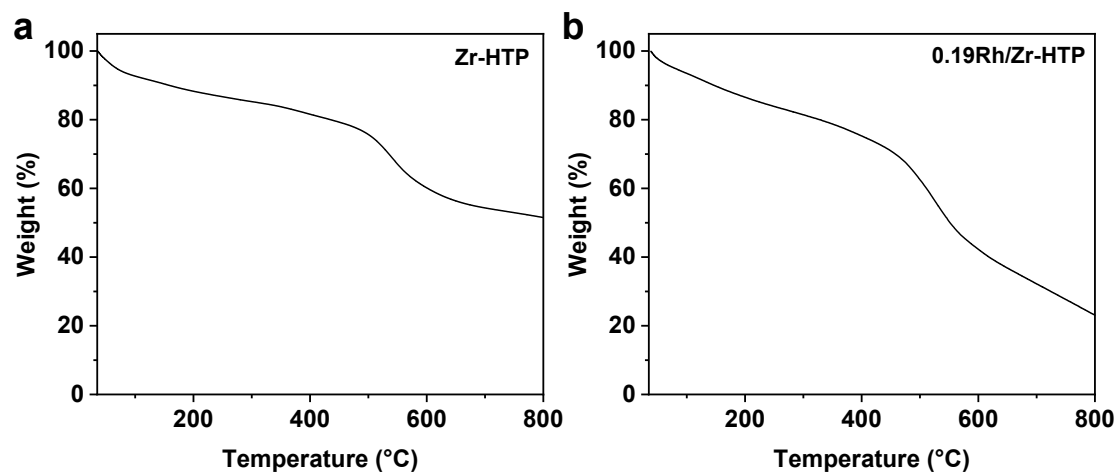


Fig. S3. TGA curves of Zr-HTP and 0.19Rh/Zr-HTP catalysts.

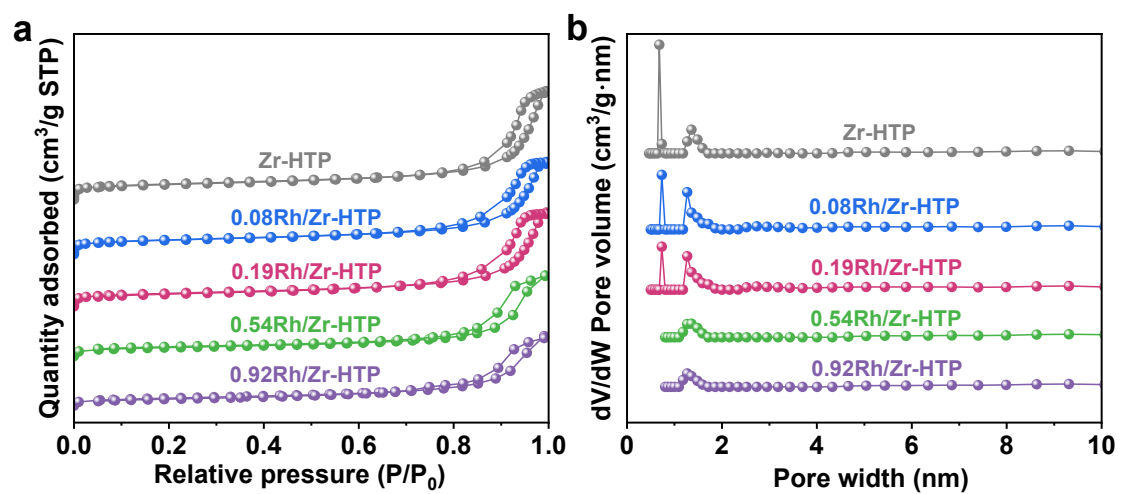


Fig. S4. N₂ sorption isotherms and pore size distributions of different Rh-based catalysts.

Table S3. Physicochemical properties of different Rh-based catalysts.

Samples	BET areas (m ² /g)	Micropore areas (m ² /g)	Pore volumes (cm ³ /g)	Micropore volumes (cm ³ /g)	Micropore ratio ^a (%)
Zr-HTP	424	173	1.03	0.072	7.0%
0.08Rh/Zr- HTP	395	151	0.87	0.063	7.2%
0.19Rh/Zr- HTP	365	145	0.90	0.059	6.5%
0.54Rh/Zr- HTP	254	33	0.79	0.010	1.3%
0.92Rh/Zr- HTP	233	24	0.70	0.007	1.0%

^a[Micropore ratio] = [Micropore volumes]/[Pore volumes]

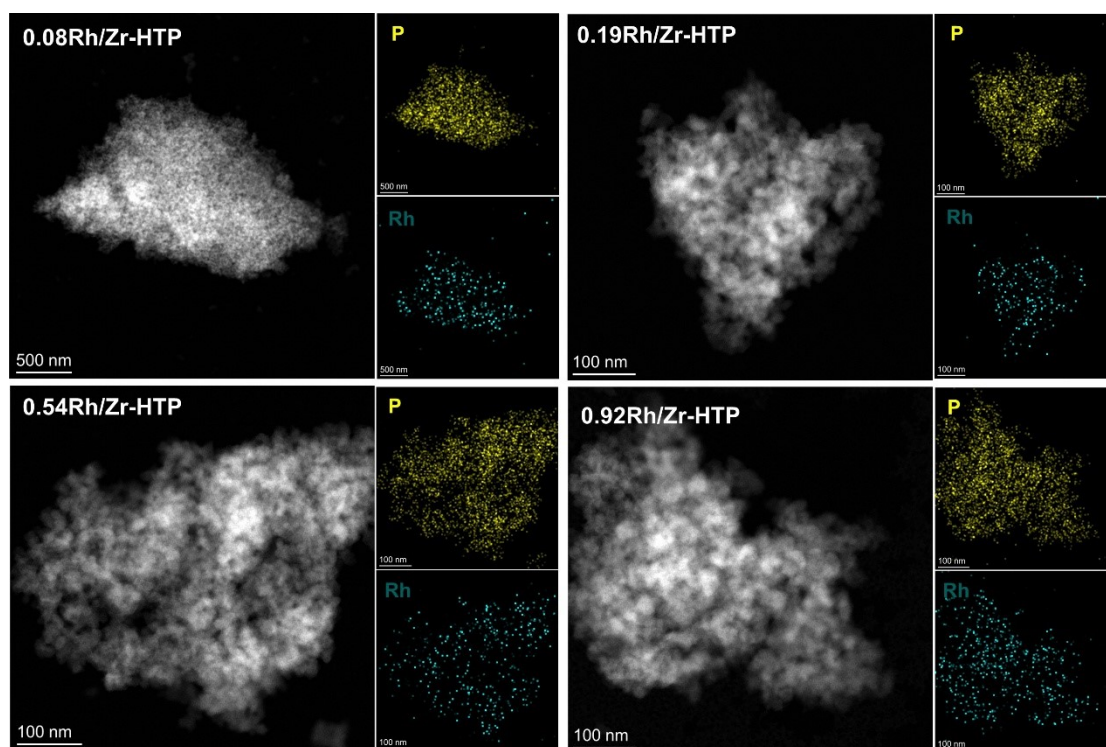


Fig. S5 The HAADF-STEM images of different catalysts and corresponding elemental mappings of Rh and P.

Table S4. Different catalysts for hydroformylation of styrene.^a

Entry	Catalysts	Con. (%)	Yield (%)		i/n
			iso-aldehyde	n-aldehyde	
1	Zr-HTP ^b	-	-	-	-
2	Rh(CO) ₂ (acac)	99	54.7	44.3	1.2
3	Rh(PPh ₃) ₃ Cl	82	42.3	39.7	1.1
4	Rh/C	80	41.1	38.9	1.1
5	0.19Rh/Zr-HTP	96	84.7	11.3	7.5

^aReaction conditions: 0.74 μ mol Rh-based catalysts, 3.0 mmol styrene, S/C= 4062, 3.0 ml toluene, 90 °C, 5.0 MPa syngas (CO/H₂= 1:1), 4 h. ^b40 mg Zr-HTP catalyst.

Table S5. ICP-OES analysis of the 0.19Rh/Zr-HTP catalysts.

Catalysts	Rh (wt%)
0.19Rh/Zr-HTP (fresh)	0.19
0.19Rh/Zr-HTP (used seven times)	0.19

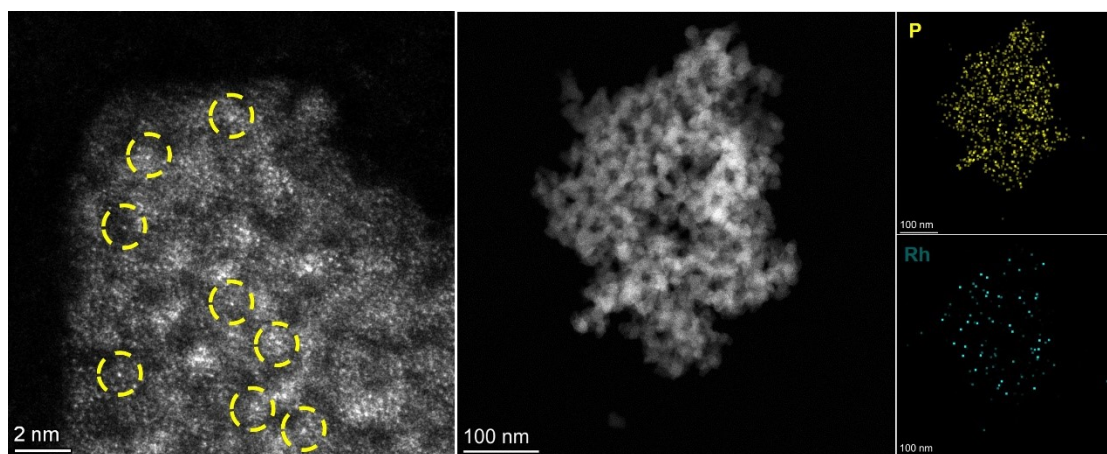


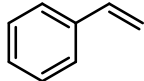
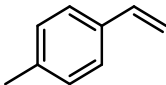
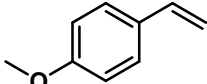
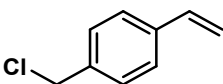
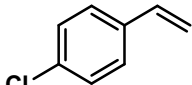
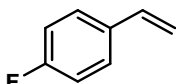
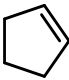
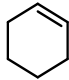
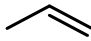
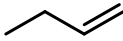
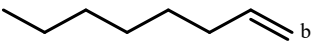
Fig. S6. The HAADF-STEM images of the spent 0.19Rh/Zr-HTP catalyst and corresponding elemental mappings of Rh and P.

Table S6. Comparison of the catalytic performance of the present catalysts with previously reported in the literature.

Catalysts	Substrate	P ^a (MPa)	T (°C)	TOF (h ⁻¹)	i/n	Ref.
Rh-HCP-PPh ₃	styrene	3.0	80	35.7	12.7	1
Rh-PPh ₃ /SiO ₂	styrene	5.0	60	239	5.7	2
2.3%Rh@POP	styrene	3.0	80	679	0.83	3
MOF-808-2.0DPPB-RhH	styrene	2.0	110	239	0.61	4
RhC _x @S-1-400	styrene	4.0	85	737	1.25	5
Rh/MnMOF	styrene	8.0	80	55.6	2.2	6
Rh/3%B-g-C ₃ N ₄	styrene	6.0	100	12000	1.32	7
Rh/ECN(0.1)	styrene	2.0	90	125	1.6	8
Rh@POP-PTBA-HA-50	1-octene	6.0	120	801	0.087	9
Rh/mPPh ₃ &PPD-POP	1-octene	2.0	110	2000	0.063	10
0.19Rh/Zr-HTP	styrene	5.0	90	1462	7.5	This work

^aCO/H₂=1:1

Table S7. Hydroformylation of various olefins under biphasic reaction conditions.^a

Substrate	Con. (%)	Yield (%)		i/n
		iso-aldehyde	n-aldehyde	
	99	87.2	11.7	7.4
	96	83.8	12.2	6.8
	84	72.6	11.4	6.4
	99	93.6	5.4	17.3
	99	86.7	12.3	7.0
	99	86.1	12.9	6.7
	26	-	26	-
	90	-	90	-
	-	46.8	48.1	1.0
	99	47.2	51.8	0.9
	99	39.3	57.7	0.7

^aReaction conditions: 40 mg 0.19Rh/Zr-HTP, 3.0 mmol olefins, S/C= 4062, 3.0 ml toluene, 90 °C, 5.0 MPa syngas (CO/H₂= 1:1), 6 h. ^bThe yield of iso-octene as byproduct was 2%.

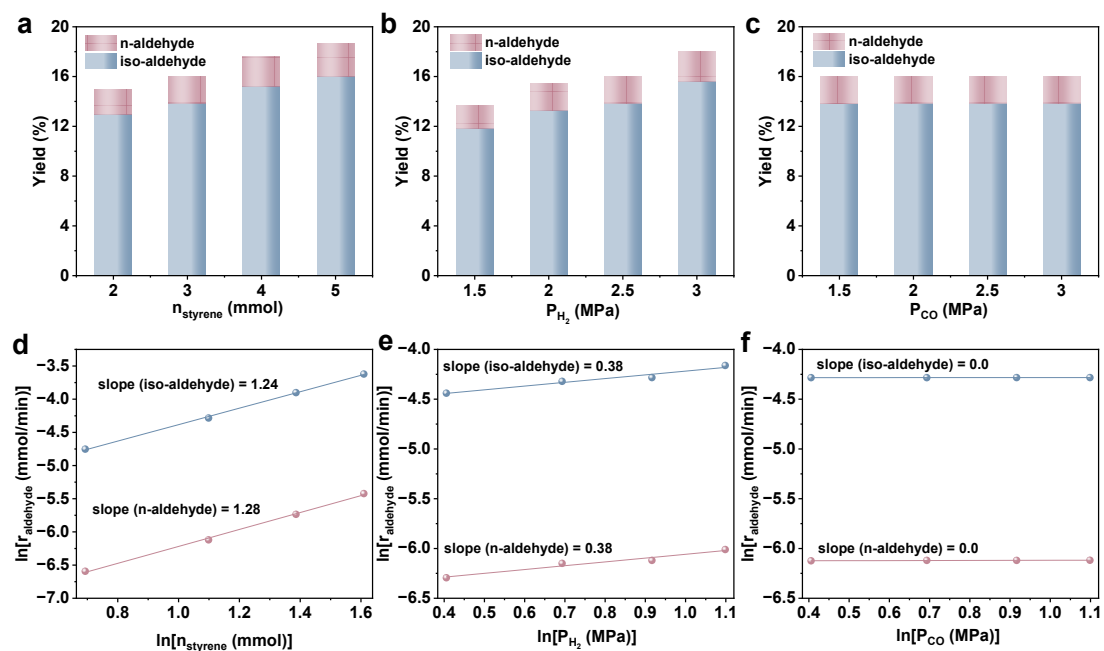


Fig. S7. Initial rate method and reaction order to the hydroformylation reaction of styrene toward (a, d) styrene, (b, e) H_2 and (c, f) CO . Reaction conditions: 40 mg 0.19Rh/Zr-HTP catalyst (0.74 μmol Rh), 3 mL toluene, 90 $^\circ\text{C}$, 30 min. (a, d) 5 MPa syngas, 2/3/4/5 mmol styrene; (b, e) 3 mmol styrene, 2.5 MPa CO , 1.5/2/2.5/3 MPa H_2 ; (c, f) 3 mmol styrene, 2.5 MPa H_2 , 1.5/2/2.5/3 MPa CO .

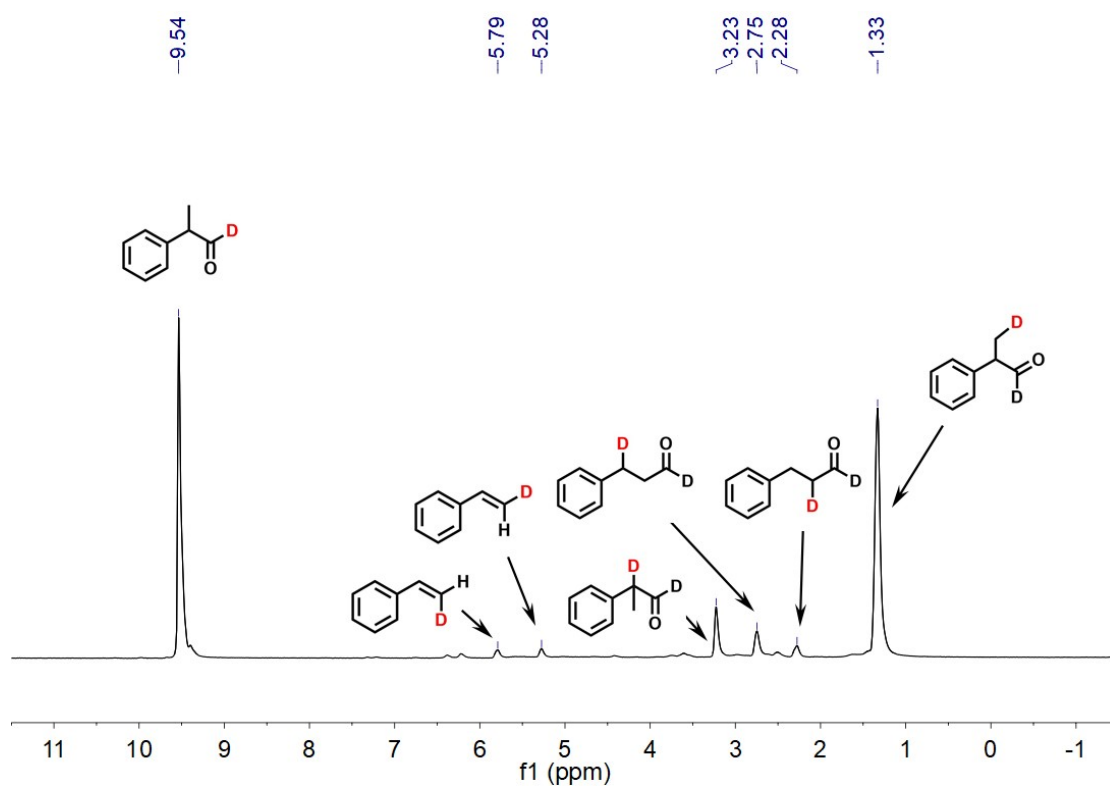


Fig. S8. ^2H NMR spectrum (600 MHz) of reaction mixture after deuteroformylation. Reaction conditions: 5.0 mmol styrene, 40 mg 0.19Rh/Zr-HTP (molar ratio of styrene/Rh=1:6770), 4.0 mL toluene, 2.5 MPa CO, 2.5 MPa D_2 , 90 °C and 6 h.

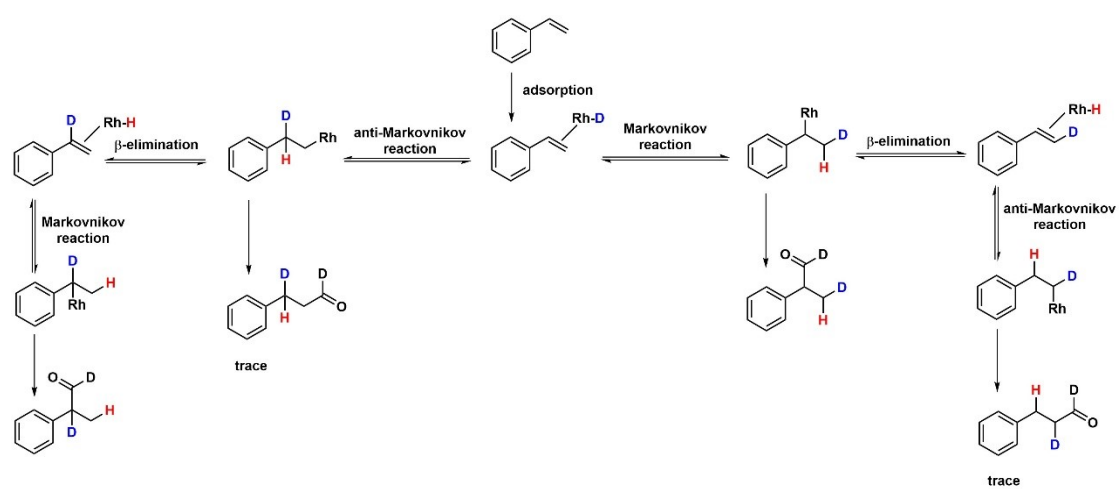


Fig. S9. Graphical representation of product distribution obtained from deuteroformylation of styrene.

Reference

- [1] D. Wang, G. Zeng, J. Fang, H. Li, H. Chen, J. Ma and Z. Dong, *Chem. Eng. J.*, 2024, **482**, 148860. DOI: 10.1016/j.cej.2024.148860.
- [2] D. Han, X. Li, H. Zhang, Z. Liu, G. Hu and C. Li, *J. Mol. Catal. A-Chem.*, 2008, **283**, 15-22. DOI: 10.1016/j.molcata.2007.12.008.
- [3] M. Xu, D. Yang, H. Fang, Z. Sun, S. Tao, S. Yang, R. Li, H. Chen, C. Cheng, X. Wang, T. Ma and X. Zheng, *J. Catal.*, 2025, **443**, 115977. DOI: 10.1016/j.jcat.2025.115977.
- [4] P. Samanta, A. Solé-Daura, R. Rajapaksha, F. M. Wisser, F. Meunier, Y. Schuurman, C. Sassoie, C. Mellot-Draznieks and J. Canivet, *ACS Catal.*, 2023, **13**, 4193-4204. DOI: 10.1021/acscatal.3c00398.
- [5] L. Huang, J. Wang, Q. Liu, P. Sun, M. Nie, G. Gao, Z. Zhao, Z. Huang and F. Li, *J. Catal.*, 2025, **447**, 116095. DOI: 10.1016/j.jcat.2025.116095.
- [6] P. Tang, S. Paganelli, F. Carraro, M. Blanco, R. Riccò, C. Marega, D. Badocco, P. Pastore, C. J. Doonan and S. Agnoli, *ACS Appl. Mater. Interfaces*, 2020, **12**, 54798-54805. DOI: 10.1021/acsaami.0c17073.
- [7] Y. Shi, G. Ji, Q. Hu, Y. Lu, X. Hu, B. Zhu and W. Huang, *New J. Chem.*, 2020, **44**, 20-23. DOI: 10.1039/c9nj05385a.
- [8] L. Jurado, J. Esvan, L. A. Luque-Alvarez, L. F. Bobadilla, J. A. Odriozola, S. Posada-Pérez, A. Poater, A. Comas-Vives and M. R. Axet, *Catal. Sci. Technol.*, 2023, **13**, 1425-1436. DOI: 10.1039/d2cy02094g.
- [9] K. Zhao, H. Wang, X. Wang, T. Li, X. Dai, L. Zhang, X. Cui and F. Shi, *J. Catal.*, 2021, **401**, 321-330. DOI: 10.1016/j.jcat.2021.08.004.
- [10] G. Ji, C. Li, P. Gao, M. Jiang, L. Ma, G. Wang, G. Hou, L. Yan and Y. Ding, *Chem. Eng. J.*, 2023, **470**, 144334. DOI: 10.1016/j.cej.2023.144334.